

THREE BUNCH ENERGY STABILIZATION FOR THE SLC INJECTOR*

J. C. SHEPPARD, I. ALMOG, P. S. BAMBADE, J. E. CLENDENIN, R. K. JOBE,
N. PHINNEY, H. SHOAEE, R. F. STIENING, AND K. A. THOMPSON

*Stanford Linear Accelerator Center
Stanford University, Stanford, California 94305*

Abstract

Slow feedback has been developed to control the energy and energy spread of the beams which are injected into the SLC damping rings. Within a single RF pulse, two bunches of electrons and one bunch of positrons are accelerated to an energy of 1.21 GeV in the injector of the SLC. The two electron bunches are deflected into the north damping ring while the positrons are targeted into the south ring. In order to fit into the acceptance of the rings, the composite energy deviation and energy spread of the beams must be less than 2% full width. Control of the beam energy characteristics is accomplished with a set of computer controlled feedback loops which monitor the parameters of the three bunches and make adjustments to the available RF energy, RF phasing, and RF timing. This paper presents an overview of the feedback algorithms and of the special hardware developments, and reports on the operational status of the processes.

Introduction

On each cycle of the SLC, the injector¹ accelerates two electron bunches and a single positron bunch to the damping ring energy of 1.21 GeV. This acceleration is accomplished within a single RF pulse because the time separation of successive bunches in the injector is about 60 ns. The composite energy spread and centroid energy deviation of each bunch must be less than the 2% energy acceptance of the damping rings.

Figure 1 illustrates the layout of the SLC injector. The hardware which is required to bring each of the three bunches into the damping ring energy acceptance is schematically shown in the figure. A pair of electron bunches, spaced by 61.6 ns, and

produced, bunched, and accelerated to about 40 MeV in the source region (CID). This pair of bunches is accelerated to an energy of about 200 MeV in the booster linac (S0) and injected into sector one through a chicane of 12° bend magnets. The energy of the electrons injected into S1 can be varied using a vernier klystron in S0. A single positron bunch is injected into sector one in the vertical plane through the last chicane magnet. Positrons are injected 55.9 ns after the second electron bunch with an energy of about 200 MeV. The energy of injected positrons is set within the e^+ production system. The three bunches are then accelerated through S1 and injected at the specified 1.21 GeV into the transport lines leading to the two damping rings (LTRs). A pulsed 15° bend (BAS 1) has been installed at the 200 MeV point to permit spectral measurements of the bunches injected into S1. Beam position monitors (BPMs), located in the LTRs, are used to determine the energy and energy spread of each of the three bunches delivered from the injector. Energy and energy spread of the bunches are controlled by adjusting the RF power, RF timing, and RF phases in the upstream accelerating sections. Vernier klystrons have been installed in both S0 and S1 to permit variation of RF power. Modulator-klystron triggers of the six SLEDded klystrons in S1 can be changed so that the bunches ride farther up or down the S1 RF envelope. Separate phase controls allow independent adjustments to the RF phase in CID, S0, and S1.

Three Bunch Energy

At the exit of S1, the energies of the first electron bunch, second electron bunch, and positron bunch are respectively given as E_{e1}^- , E_{e2}^- , and E_{e3}^+ :

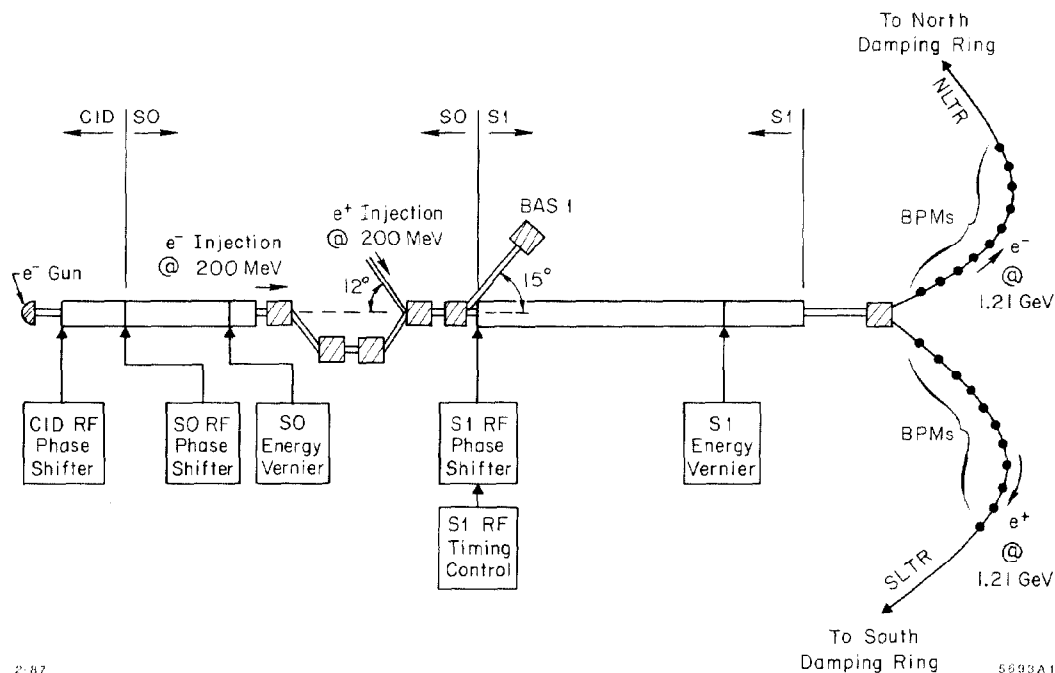


Fig. 1. Overview of the SLC injector showing the separate RF phase, energy, and timing controls necessary for energy stabilization.

* Work supported by the Department of Energy, contract DE-AC03-76SF00515.

$$E_{o1}^- = E_{I1}^- + V_1 \times \text{SLED}(t_1) \cos(\phi_1) - \Delta_{11}(N_1)f(\sigma_{z1}) \quad (1a)$$

$$E_{o2}^- = E_{I2}^- + V_1 \times \text{SLED}(t_2) \cos(\phi_2) - \Delta_{22}(N_2)f(\sigma_{z2}) - \Delta_{21}(N_1) \quad (1b)$$

$$E_{o3}^+ = E_{I3}^+ + V_1 \times \text{SLED}(t_3) \cos(\phi_3) - \Delta_{33}(N_3)f(\sigma_{z3}) - \Delta_{32}(N_2) - \Delta_{31}(N_1) \quad (1c)$$

wherein

$$E_{I1}^- = V_I \cos(\phi_1) - \Delta_{I11}(N_1)f(\sigma_{z1}) \quad (2a)$$

$$E_{I2}^- = V_I \cos(\phi_2) - \Delta_{I22}(N_2)f(\sigma_{z2}) - \Delta_{I21}(N_1) \quad (2b)$$

In Eq. (1), E_{Ij} is the energy of the j^{th} bunch at the beginning of S1; ϕ_j is the phase of the j^{th} bunch with respect to the crest of the RF; V_1 is the noload energy gain contribution of the six S1 klystrons; $\text{SLED}(t)$ is the SLEDded² RF energy envelope as a function of time; t_j is the time at which the j^{th} bunch is injected into S1; Δ_{jk} is the beamloading decrease in available S1 energy for the j^{th} bunch due to the presence of the k^{th} bunch; N_j is the number of particles in the j^{th} bunch; and f is a bunch length (σ_z) dependent amplitude factor which affects the magnitude of the intrabunch beamloading (Δ_{jj}); $\Delta_{I,jk}$ is the corresponding beamloading in the CID and S0 accelerator sections; and V_I is the noload energy gain of the nonSLEDded CID and S0 sections. Table 1 lists the nominal values of the aforementioned parameters.

Table 1. Nominal Values

Parameter	Description	Nominal value
E_{I1}^-	Injected e_1^- energy	0.200 GeV
E_{I2}^-	Injected e_2^- energy	0.200 GeV
E_{I3}^+	Injected e_3^+ energy	0.200 GeV
V_I	Available injector energy	0.275 GeV
V_1	Available sector 1 energy	1.136 GeV
ϕ_j	Mean phase wrt RF	see figure 5
SLED	SLED pulse shape	see figure 2
t_j	Time of bunch wrt SLED peak	t_1 $t_2 = t_1 + 61.6$ ns $t_3 = t_1 + 117.6$ ns
$\Delta_{I11}(N), \Delta_{I22}(N)$	Intrabunch loading	$0.0047 \frac{N}{5 \times 10^{10}}$ GeV
$\Delta_{I21}(N)$	Interbunch loading	$0.0043 \frac{N}{5 \times 10^{10}}$ GeV
$\Delta_{jk}(N)$	Intrabunch loading	$0.029 \frac{N}{5 \times 10^{10}}$ GeV
$\Delta_{21}(N), \Delta_{32}(N)$	Interbunch loading	$0.027 \frac{N}{5 \times 10^{10}}$ GeV
$\Delta_{31}(N)$	Interbunch loading	$0.025 \frac{N}{5 \times 10^{10}}$ GeV
$f(\sigma_z)$	Intrabunch loading form factor	see figure 3
σ_z	RMS bunchlength	2 mm for e^- 3 mm for e^+

From Eq. (1) it is seen that the energy of a bunch at the end of S1 depends primarily on the energy at which it was injected into S1, the available RF voltage (V_1), the intrabunch beamloading (Δ_{jj}), and the beamloading due to the passage of previous bunches (Δ_{jk}). The variation of energy gain due to the SLED envelope is shown in Figure 2. The beamloading terms are current dependent and there is a slight dependence of the self loading term on bunch length, $f(\sigma_z)$. A plot of $f(\sigma_z)/f(2 \text{ mm})$ is shown in Figure 3. Whereas the value of ϕ_j affects the bunch energy, the most important effect of ϕ_j is on the energy spread. Figure 4 illustrates the variation in energy spread with ϕ_j for $\sigma_z = 2 \text{ mm}$ and $\sigma_z = 3 \text{ mm}$ at a current of $N = 5 \times 10^{10}$ particles per bunch. The value of ϕ_j , which minimizes energy spread, is shown in Figure 5 as a function of current for several different values of bunch length.

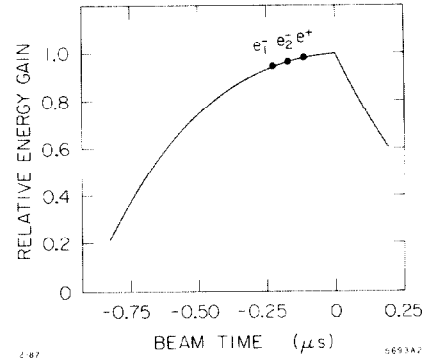


Fig. 2. Relative energy gain of the S1 SLEDded RF wherein the relative timing of the three injector bunches is indicated.

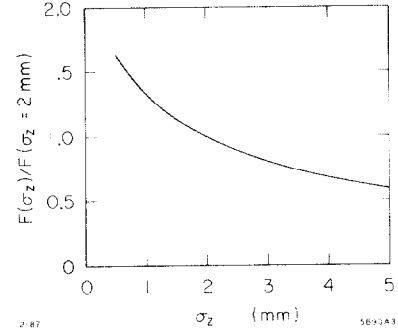


Fig. 3. Dependence of the magnitude of intrabunch beamloading on the bunch length (σ_z).

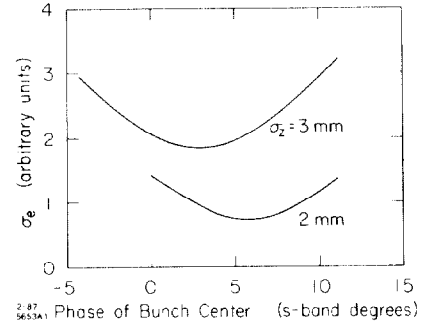


Fig. 4. Variation of energy spread with RF phase.

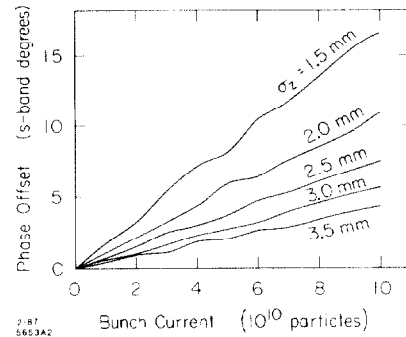


Fig. 5. Phase required to minimize energy spread as a function of the number of particles per bunch for different values of bunch length (σ_z).

Energy Error Detection

BPM readings in the LTRs are analyzed to deduce deviations in bunch energy from a reference orbit.³ The change in horizontal position from the reference orbit, X_0 , is given as δX :

$$\delta X \equiv X - X_0 = D_x \frac{\delta E}{E_0} + R_{11} \delta X_i + R_{12} \delta X'_i \quad (3)$$

where X is the measured horizontal position; D_x is the horizontal dispersion; δE is the energy deviation from the reference energy, E_0 ; δX_i and $\delta X'_i$ are the changes in initial horizontal position and angle; and R_{11} and R_{12} are the usual Transport⁴ R matrix elements referenced to the beginning of the transport line. Measurements of δX at three different monitors are sufficient to solve Eq. (3) for the deviations δE , δX_i , and $\delta X'_i$. Errors in the deduced energy deviation are reduced by averaging over many BPMs for several (~ 5) beam pulses. In practice, 17 different BPMs in the first third of each LTR are used to measure δE . Large energy excursions ($\delta E/E_0 \geq 1\%$) can result in a distributed beam loss which perturbs the monitor readings. This ultimately leads to calculation of erroneous values of δE , δX_i , and $\delta X'_i$. The impact of such errors tends to be minimized by feeding back only on the energy error; the energy corrections based on Eq. (3) converge in virtually all cases.

Bunch energy spread is determined by using several BPMs in each LTR to measure the quadrupole moment of the beam, Q .⁵ At a location with horizontal dispersion, D_x , Q is given by:

$$Q = D_x^2 \sigma_e^2 + \sigma_{\beta x}^2 - \sigma_y^2 + \langle x \rangle^2 - \langle y \rangle^2 \quad (4)$$

where σ_e is the energy spread; $\sigma_{\beta x}$ is the horizontal beam size in the absence of energy spread; σ_y is the vertical beam size; and $\langle x \rangle$ and $\langle y \rangle$ are the horizontal and vertical beam positions.

$$P = Q - (\langle x \rangle^2 - \langle y \rangle^2) \quad (5)$$

is calculated in the LTR microprocessor and sent off to the central control system computer. The main computer is used to vary the RF phase to minimize P . Problems associated with noisy P signals are reduced by averaging P at a constant phase setting for a number (~ 10) of beam pulses. Reliable determination of the phases which minimize P are found by fitting a parabola to the measured P versus phase data.

Hardware For Energy Compensation

The accelerating voltages V_I and V_1 are adjustable on a pulse to pulse, beam code dependent basis using vernier klystrons in S0 and S1.⁶ Figure 6 illustrates the control circuit. A variable attenuator is adjusted through the computer to change the drive to the klystron, which is operated out of saturation. Klystron power output as a function of attenuator setting is first calibrated, using a phase and amplitude detector, to determine the attenuator drive to beam energy gain transfer function. This transfer function is subsequently used to set the available energy output of the tube to the desired value. Klystrons are presently being varied from fully off up to saturation. Variability in energy output is 0-50 MeV for the S0 klystron and 0-165 MeV for the S1 tube.

RF phase adjustments are made by varying the sector sub-booster phase shifters⁷ which change the phase of the drive applied to each klystron in a sector. The CID phase shifter moves the phase of the subharmonic bunchers and S-band buncher as well as of the accelerating section. A new module has recently been installed that will also shift the gun timing along with the phase so that the bunching process will be undisturbed.

RF timing adjustments in S1 are accomplished by shifting the subbooster drive and SLED phase reversal along with the modulator firing times. Timing shifts of the unSLEDded klystrons of CID and S0 are not necessary.

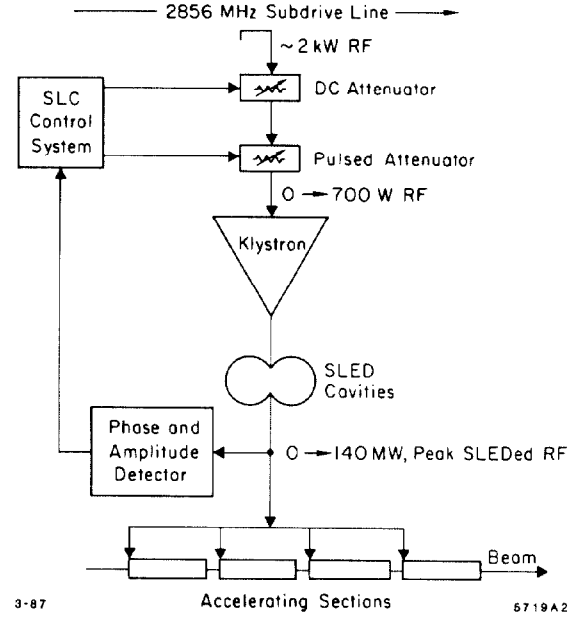


Fig. 6. Energy output of a vernier klystron is adjusted by varying the input drive with a pulsed attenuator. A phase and amplitude detector is used to calibrate the system.

Computer Controlled Feedback

Slow, computer controlled feedback^{8,9} has been written to stabilize the energy at the end of the SLC injector. Five orthogonal loops have been designed to control the various three bunch energy characteristics. In general, the loops are scheduled on an independent basis. Each loop calls a launch error routine to measure the parameter of interest. If the measured signal value is outside of the setpoint tolerance, a command is sent to a particular device or group of devices to correct the error while leaving the other energy parameters unperturbed. A damping factor is included in the process so that only a fraction of the desired correction is applied on each iteration.

After the three bunches have been established, the following algorithms are used to stabilize the energy parameters. The energy of the first electron bunch is corrected by adjusting the energy contribution from the S0 vernier klystron. The energy difference of the second electron bunch with respect to the first is nulled by varying the S1 SLEDed RF timing. Compensation for overall energy changes due to S1 timing shifts is accomplished by feeding forward with the S1 vernier klystron. Composite energy spread of the two electron bunches is minimized by shifting the phase at which the electrons are accelerated through S0 and S1. This phasing adjustment is made by varying the CID RF phase shifter. Net energy changes associated with the CID phase shift are compensated by using the S0 vernier. The energy of the positron bunch is controlled by varying the energy contribution of the S1 vernier klystron. Compensating changes to the S0 vernier klystron are made so that the electron energies are not varied when positron energy is corrected. The energy spread of the positrons is minimized by moving the RF phase of S1. The phases of CID and S0 are moved in concert with S1 so that the overall RF phase seen by the electrons remains unchanged.

Status and Future Work

All of the associated energy stabilization hardware has been installed, tested, and integrated into the SLC control system. All of the control and feedback software has been written. The software routines responsible for data acquisition and energy error determination have all been tested and debugged. As of March 1987, electron and positrons are being accelerated through the injector on separate RF pulses so that only a subset of the full energy stabilization feedback has been required and tested.

Centroid energy stabilization for single bunch injection into either of the two LTRs is commissioned. Since the energy verniers are controllable on a pulse by pulse basis, only the S1 vernier is presently being used for energy control into either LTR. The centroid stabilization loop has been running continuously since June 1986.

Energy spread minimization has been commissioned for electron injection into the north LTR. Since positrons were not available during commissioning of this loop, it was decided to vary only the S1 RF phase to minimize the energy spread. However, the controls are in place to vary the upstream (CID and S0) phases as well. The energy spread detection hardware in the south LTR has been tested using electrons and is currently integrated into the control system. At this time, the energy spread does not vary significantly so the minimization loop is usually not operated.

Centroid energy stabilization of pairs of electron bunches has been commissioned. As in the case of the single bunch stabilization, only the S1 energy vernier is being used in conjunction with the S1 RF timing shifts. At present, routine two electron bunch operation is pending the installation of a fast two bunch extraction kicker for the north damping ring. Thus, only limited operating experience has been gathered with this feedback loop.

Positron energy stabilization is currently under operator control using the pulsed S1 energy vernier. Computer feedback for positron centroid energy stabilization will be turned on as soon as the proper positional launch into the south LTR has been achieved. Positron energy spread is also presently under operator control using a pulsed phase shifter connected in series with the S1 RF.

Commissioning of the positron with electron energy feedback is awaiting the co-acceleration positrons and electrons through the injector. Plans call for initially bringing up energy stabilization for single electron bunches accelerated with the positron bunch. Once this has been tested and debugged, commissioning of the full three bunch stabilization will begin.

Acknowledgments

It is a pleasure to acknowledge the contributions of Wm. Allen and H. Schwarz in regards to the hardware necessary for the control and monitoring of the RF. M. Flores, T. Gromme, L. Sanchez, K. Underwood, and M. Woodley have made significant contributions to the software. As always, we acknowledge the contribution of M. Ross and the main control operators who participate in all phases of the energy stabilization system commissioning.

References

1. J. C. Sheppard *et al.*, "Commissioning of the SLC Injector," these Proceedings.
2. Z. D. Farkas *et al.*, "SLED: A Method of Doubling SLAC's Energy," Proc. 9th Int. Conf. on High Energy Accel., Stanford, CA, 1974, p. 576.
3. I. Almog *et al.*, "Model-Based Trajectory Optimization for the SLC," these Proceedings.
4. K. L. Brown *et al.*, "TRANSPORT, A Computer Program for Designing Charged Particle Beam Transport Systems," SLAC-91 (Rev. May 1977).
5. J. C. Sheppard *et al.*, "Implementation of Nonintercepting Energy Spread Monitors," these Proceedings.
6. R. K. Jobe *et al.*, "Computer Control of the Energy Output of a Klystron in the SLC," these Proceedings.
7. H. D. Schwarz, "Computer Control of RF at SLAC," IEEE Trans. Nucl. Sci. NS-32, 1847 (1985).
8. K. A. Thompson *et al.*, "Feedback Systems in the SLC," these Proceedings.
9. R. K. Jobe *et al.*, "Position, Angle and Energy Stabilization for the SLC Positron Target and Arcs," these Proceedings.